Article citation info:
Mielcarzewicz D, Szwajca F, Pielecha I. Combustion and emissions of a hydrogen-ammonia mixture engine with passive and active turbulent jet ignition. Combustion Engines. 0000;XXX(X):xx-xx. https://doi.org/10.19206/CE-222665

Dawid MIELCARZEWICZ
Filip SZWAJCA
Ireneusz PIELECHA

Combustion Engines
Polish Scientific Society of Combustion Engines

Combustion and emissions of a hydrogen-ammonia mixture engine with passive and active turbulent jet ignition

ARTICLE INFO

Received: 7 February 2026
Revised: 24 May 2026
Accepted: 29 May 2026
Available online: 23 June 2026

The search for fossil fuel substitutes has led to the adoption of carbon-free alternatives, such as hydrogen and ammonia. It is also possible to use mixtures of both these fuels. Due to their different physical and chemical properties, the combustion processes of hydrogen and ammonia differ. The paper describes research on hydrogen and hydrogen-ammonia mixture combustion in the AVL 5804 engine. The engine is equipped with a two-stage combustion system with a passive and active prechamber. During the study, an indicator analysis of the combustion process in the prechamber and main chamber was performed. The study also included an evaluation of changes in hydrogen and nitrogen oxides concentrations, as well as changes in the number of particulate matter particles in the exhaust gases. By comparing the combustion of hydrogen and hydrogen-ammonia mixtures, it was observed that the thermodynamic parameters of the combustion process changed, along with emissions of unburned hydrogen and nitrogen oxides. However, there were insignificant differences in the number of particulate matter.

Key words: *hydrogen and ammonia combustion, Turbulent Jet Ignition system, hydrogen emission, PN emission*

1. Introduction

The development of internal combustion engines is focused on reducing carbon dioxide emissions to reduce the greenhouse effect. Currently, the possibility of implementing carbon-free fuels to partially replace conventional fuels is being explored. The main solution in this case is hydrogen, but its low volumetric energy density has led to research on ammonia.

To fully leverage the potential of these fuels, efforts are underway to improve combustion efficiency. Since these are gas fuels, it is advantageous to burn lean mixtures with a relatively high compression ratio [17]. Hydrogen-powered engines commonly operate at compression ratios of $\varepsilon = 11–15$ [22, 23], whereas ammonia-powered engines require higher compression ratios of $\varepsilon = 20$ and above [15, 16]. The combustion of lean air-fuel mixtures with hydrogen occurs at significantly higher excess air ratios than with conventional gaseous fuels. To avoid knock combustion, hydrogen engines operate at an excess air ratio above 2 [8–10, 24]. In addition to increasing the mixture's dilutions, adding ammonia can reduce knock combustion by limiting charge reactivity [8].

2. Characteristics of hydrogen and ammonia combustion conditions

The combustion of hydrogen enables replacing conventional fossil fuels, provided certain requirements are met. Hydrogen as a fuel requires, among other things, a modernized dose supply system (usually to the intake manifold) or direct injection [31]. The use of such solutions enables precise control of the mixture composition in a wide range of excess air ratios. Using the TJI system, which involves indirect hydrogen injection into the intake manifold and additional direct injection into the prechamber, it is possible to significantly extend the limits of stable combustion towards lean mixtures. The use of APC (active prechamber) or PPC (passive prechamber) results in stable hydrogen combustion at $\lambda = 3$ [27]. Hydrogen and ammonia combustion can be carried out in single-fuel [3, 17, 19], dual-fuel systems [26] or using mixtures of these fuels [26, 28] (Table 1).

The laminar combustion velocity increases with the mixture temperature, due to faster chemical reaction kinetics and higher diffusion rates of active radicals. Research conducted by Guibert et al. [7] indicates significant differences in the combustion velocity of hydrogen and ammonia: at a temperature of 500 K, this velocity is approximately 2 m/s (for hydrogen) and 0.07 m/s for pure ammonia. A mixture of H_2:NH_3 in the 20:80 ratio has a laminar combustion velocity of 0.1 m/s.

The impact of EGR on the combustion process in a hydrogen-powered engine was analyzed by Pandey et al. [20]. During research, a single-cylinder engine with a displacement of 0.661 dm^3 and a compression ratio of 15 was used. The use of a 15% EGR additive results in:

- a slight decrease in thermal efficiency (from 30.5% to 29%)
- a delay in the start of combustion by approximately 2 degrees
- an extension of the combustion time by approximately 2 degrees
- a reduction in nitrogen oxide emissions from 10 to 8 g/kWh. Increasing the EGR ratio to 25% limits these emissions to 2 g/kWh.

The reaction of the $H_2 + NH_3$ combustion proceeds according to the equation:

$$3H_2 + 2NH_3 + 3O_2 \rightarrow N_2 + 6H_2O \quad (1)$$

Research [15] indicates that under stoichiometric conditions, an optimal ammonia-to-fuel mass ratio of 0.6 balances emissions and fuel consumption. Empirical studies also indicate that increasing hydrogen's energy share relative to ammonia may initially improve thermal efficiency.

Table 1. Physical and chemical properties of fuels [4, 10, 19]

Fuel	H_2	NH_3	$H_2 + NH_3$ (95% + 5%) m/m
Weight of H_2 [%]	100	17.7	–
Auto-ignition temp. [°C]	773	923	–
Boiling point [°C]	–253.0	–33.4	–
LHV [MJ/kg]	120	18.6	114.93
LHV [MJ/m^3]	2.90	2.83	–
Flammability limit [%]	4–75	15–28	–
Laminar flame speed [m/s]	1.6	0.07	–
Minimum ignition energy [mJ]	0.02	8	–
Liquid density [g/cm^3]	0.08 (–253°C)	0.68 (–33.4°C)	–

The combustion of ammonia leads to an increase in the concentration of nitrogen oxides due to their formation from both fuel and air – Zeldovich mechanism (Fuel NO_x and Thermal NO_x) [9, 16]. In contrast, hydrogen combustion only forms NO_x via the Thermal-NO_x mechanism (Fig. 1).

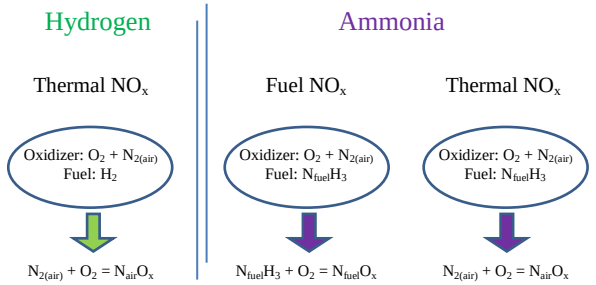

Fig. 1. The mechanism of NO_x formation as a result of hydrogen and ammonia combustion (based on [3, 9, 16])

Due to the dual nature of NO_x formation during ammonia combustion, it can be concluded that a significant portion of NO_x is formed as thermal-NO_x, approximately 70% (at an excess air ratio of $\lambda = 1$) [16]. Increasing the leanness of the mixtures increases the proportion of thermal-NO_x; for example, the NO_x concentration in mixtures with $\lambda = 1.6$ is about 7 times higher.

Research conducted by Pyrc et al. [24] indicates that reducing the volume fraction of hydrogen to 7% in a mixture with ammonia enables the highest indicated efficiency of 27.6% (at $\varepsilon = 10$) to be achieved in an engine at n = 600 rpm and $\lambda = 1.06$. The high hydrogen fraction in the mixture (70%) resulted in a slightly lower indicated efficiency of 24.8%. However, nitrogen oxide emissions were reduced by a factor of 4 (from 26.7 to 7.7 g/kWh) during combustion of a fuel with a low hydrogen fraction.

In studies conducted by Mounaïm-Rousselle et al. [18], it was found that adding only 10% hydrogen to ammonia reduces nitrogen oxides emissions by 40% (in a standard combustion system). A smaller addition of H_2 – 2.2% at $\lambda = 1$ (standard combustion system) causes an increase in NO_x concentration from 10 to 80% (as a result of advancing or delaying the ignition angle) [11]. This may be because the ignition temperature and pressure are high near TDC, which consumes OH radicals too quickly and inhibits NO_x formation, whereas when the ignition timing is far from TDC, NO_x emissions increase.

Most of the studies mentioned above concern mixtures containing a significant proportion of ammonia and hydrogen. Research on mixtures of hydrogen with a small proportion of ammonia has been conducted by, among others, Xin et al. [33]. The tests were conducted with 5%, 8% and 10% of ammonia added, at an excess air ratio of $\lambda = 1$. As the ammonia proportion increased, the rate of pressure rise after ignition decreased by 15%. The extension of the initial combustion period of the mixture (CA0–10) was also around 15%. However, an increase in the IMEP value of around 5% was observed, regardless of the ignition angle and a few percent reduction in the ITE. The change in ammonia volume fraction had a minor effect on the final nitrogen oxide concentration values, but an increase was observed when the ignition timing was delayed.

Further research by Xin et al. [34] investigated the effects of ammonia concentrations of 0% and 2.2% under lean-burn conditions ($\lambda = 1.2$). A slightly leaner mixture reduced the rate of pressure rise by around 10%, regardless of ignition timing. Similar values were obtained for the increase in the first combustion phase (CA0–10), although these were strongly dependent on the ignition angle. The addition of ammonia significantly increased NO_x concentrations, but this increase depended slightly on the ignition angle.

An overview of the overall TJI process is summarised in Fig. 2, including the key parameters and physical process. In general, the jet ignition process is divided into three phases: prechamber combustion, cold-jet and jet ignition, and lean combustion [35].

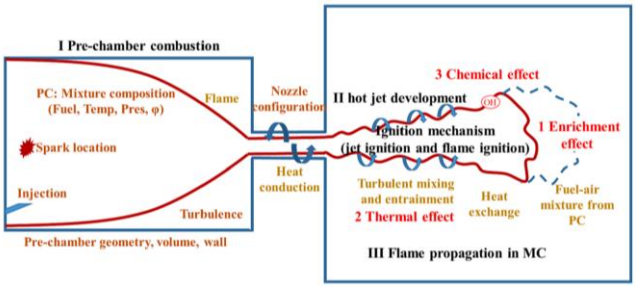

Fig. 2. Overview of TJI process. The injection only symbolises the act of fuel injection, and it does not indicate the actual position and directions of injection [36]

3. Purpose and scope of research

Modern combustion systems with a prechamber are being intensively researched for the use of hydrogen and ammonia fuels. This paper describes the use of a Turbulent Jet Ignition (TJI) system with a passive (PPC) and active prechamber (APC), enabling stable combustion of globally lean mixtures.

The aim of the work was to analyze the combustion process of hydrogen and hydrogen-ammonia fuels in the TJI engine with PPC and APC configurations. The test included analysis of pressure profiles in the cylinder and emissions of unburned H_2, NO_x, and particulate matter. The research was conducted under the following conditions:

– PC (pre-chamber): supplied with hydrogen
– MC (main-chamber): supplied with hydrogen or a mixture of hydrogen (95% m/m) and ammonia (5% m/m)

– $\lambda > 2.0$ for hydrogen and $\lambda > 1.5$ for a mixture of H_2 + NH_3
– variable fuel supply to the prechamber (t_PC = 0, 4, 8 ms).

The use of a 95%/5% H_2/NH_3 mixture is based on a comprehensive analysis of the authors previous research, which focused exclusively on fuelling the TJI engine (active and passive prechamber) with hydrogen. Further work involves adding ammonia (this article refers only to small proportions). The aim for future research is to increase the proportion of ammonia to around 50%. This approach will enable an analysis of the impact of ammonia on the combustion process, including an examination of the exhaust emissions from such systems.

4. Methodology

During the study, a single-cylinder research engine, AVL5804, was used; its technical data are presented in Table 2. The engine was equipped with a two-stage combustion system with an H_2 or H_2 + NH_3 injection system (95%/5%) into the intake manifold and direct injection into the prechamber (H_2).

The tests were conducted at a constant 1400 rpm engine speed using an independently electrically driven supercharger, allowing for adjustment over a wide range. The AVL5804 engine (Fig. 3) was powered by two independent fuel systems, each equipped with a thermal flow meter. Fuel was injected into the intake manifold at 7 bar and into the prechamber at 3 bar.

An AVL IndiSmart device was used to record rapidly changing pressure waves in the cylinder, and data from mass flow meters (hydrogen, H_2/NH_3 mixture, and air) were recorded. Detailed technical data of the equipment and the configuration of the measurement systems are presented in Table 3. In addition, the throttle position and spark timing parameters were analysed.

Table 2. AVL5804 engine specifications

Parameter	Unit	Value
Engine	–	1-cyl., 4-valve, SI, TJI
Displacement	dm^3	0.5107
Bore × stroke	mm	85 × 90
Compression ratio	–	15.5
Combustion system		Pre-chamber with 2.29 cm^3 volume and 6×1.7 mm nozzles configuration
Fueling		PFI (EM injectors); passive/active pre-chamber
Air system		External supercharger
Dyno		AMKASYN AVL AMK DW13-170

Two thermal flow meters were used to analyze hydrogen consumption and the hydrogen-ammonia mixture. Mass measurements from both flow meters enable the calculation of the excess air ratio (with simultaneous measurement of mass flow of air).

The combustion of hydrogen and a hydrogen-ammonia mixture was tested using the same injection system settings. The injection time into the main chamber was 6.5 ms, while the injection time into the prechamber was varied from 0 to 8 ms. Using identical control system settings for both fuels meant that the air excess ratio λ was a result rather than an input. The initial combustion conditions for both fuels are summarised in Table 4.

The recorded pressure profiles in the main chamber and prechamber were analysed. The indicated mean effective pressure was determined depending on the change in λ.

The assessment of the combustion system was also based on determining the indicated efficiency of each analysed point of engine operation, by the equations:

$$\eta_i = \frac{1}{g_i \cdot L_{HV}} \tag{2}$$

where L_{HV} is the lower heat value, g_i is a specific fuel consumption, calculated as:

$$g_i = \frac{G_{MC}}{N_i} \tag{3}$$

where G_{MC} is fuel consumption in the main chamber, and N_i is the indicated power:

$$N_i = \frac{V_s \cdot p_i \cdot n}{\tau} \tag{4}$$

where V_s is the displacement of the cylinder, n is the engine speed, and $\tau = 2$ (4-stroke engine).

Table 3. Control and measurement equipment

System	Name	Value
Indicating system	AVL IndiSmart	8-canal, 0.1 deg CA; crank angle AVL 365C
Oil and water conditioning	AVL 577	0–150°C
PC pressure	Kistler M3.5 6081 AQ22	0–25 MPa
MC pressure	AVL GH14D	0–25 MPa
Throttle	Bosch ETB 32 mm	±0.5 deg
Ignition	ECU Master EMU Black	0.1 deg
MC injection timing	Mechatronika	0–20 ms; ±0.1 ms
PC injection timing	Mechatronika	0–20 ms; ±0.1 ms
PC fuel flowmeter	Bronkhorst 111AC-70K	0.4–100 nl/h; accuracy ±0.1% FS
MC fuel flowmeter	Bronkhorst F-112AC	0.02–1 kg/h; accuracy ±0.1% FS
Air flow meter	ABB SensyFlow	0–720 kg/h; error < ±0.8%
H_2, NO_x concentration	E-com D	±10 ppm; ±5%
TSI EEPS 3090	Particle Number	5.6–560 nm 16 channels per decade (5.6–56 nm and 56–560); 32 total

a) b)

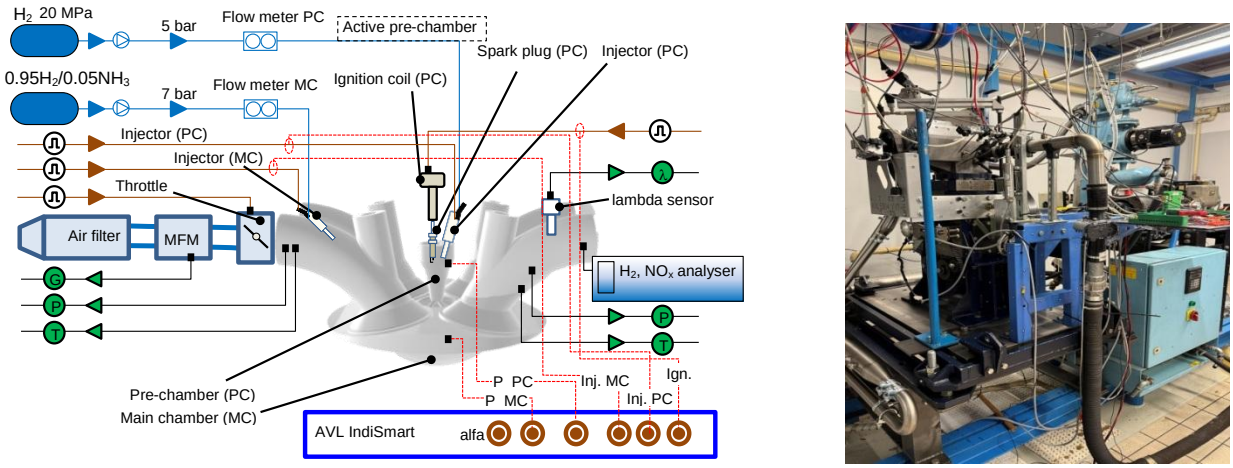

Fig. 3. The test bench: a) diagram with measurement equipment; b) view of the engine

Table 4. Injection system settings and initial λ obtained at PPC

Fuel PC/MC	H_2/H_2	$H_2/(H_2 + NH_3)$
Injection time: MC	6.5 ms	7.5 ms
Injection time: PC	0/4/8 ms	0/4/8 ms
Base lambda-value (passive PC)	2.15 2.79	1.91 2.51

The injection time measurement into the prechamber shown in Table 4 does not account for the fuel dose. For this reason, Fig. 4 shows the conversion of the prechamber injection time into the mass fraction of the total fuel dose delivered to the cylinder.

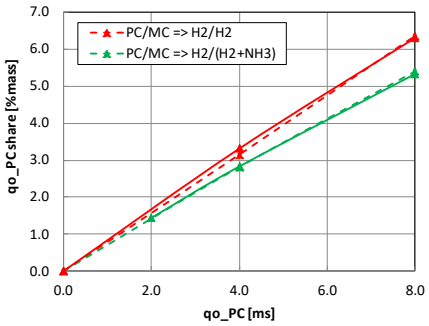

Fig. 4. Conversion of injection duration into the proportion of fuel injected into the prechamber

The plan for research on the combustion of hydrogen and a mixture of hydrogen-ammonia is shown in Table 5.

Table 5. Research plan for the combustion of hydrogen and ammonia

No.	Fuel (MC/PC)	λ-value	PC [g/h]	MC [g/h]
1	H_2/H_2	2.14	0	0.182
2	H_2/H_2	2.06	5.92	0.182
3	H_2/H_2	1.96	12.37	0.182
4	H_2/H_2	2.79	0	0.183
5	H_2/H_2	2.69	6.27	0.183
6	H_2/H_2	2.57	12.32	0.183
7	H_2/NH_3	1.91	0	0.214
8	H_2/NH_3	1.88	6.2	0.214
9	H_2/NH_3	1.83	12.22	0.214
10	H_2/NH_3	2.51	3.14	0.215
11	H_2/NH_3	2.44	6.26	0.215
12	H_2/NH_3	2.43	12.11	0.215

5. Comparison of hydrogen and hydrogen with ammonia combustion

5.1. Evaluation of indicated pressure changes

The analysis of the static test conditions (n = 1400 rpm; IMEP = 3.77 bar – a value calculated on the base of 100 subsequent engine cycles; P_max = 42.7 bar) included an evaluation of the combustion pressure profiles for the use of passive and active prechamber. The IMEP and CoV(IMEP) values are shown in Fig. 5.

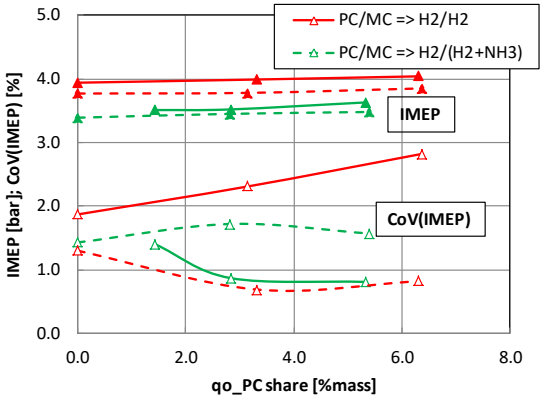

Fig. 5. The IMEP value and engine irregularity

An analysis of the uneven engine operation shows CoV(IMEP) values below 3%. This is acceptable for a single-cylinder engine. Based on the results, it can also be concluded that the use of an H_2 + NH_3 mixture reduces engine running irregularities as the fuel dose into the prechamber is increased.

The combustion of hydrogen and its mixture with ammonia using a passive prechamber was characterized by the lowest maximum combustion pressure (Fig. 6). Due to the initiation of combustion in the prechamber, a characteristic pressure peak is observed in it. Increasing the fuel dose to the prechamber (4 and 8 ms) increased combustion pressure in both the prechamber and the main chamber, with a simultaneous increase in the prechamber pressure peak amplitude.

The center of combustion (CA50) is currently an indicator of combustion efficiency. Many researchers define the optimal CA50 value as being between 6°CA and 10°CA aTDC [5, 22, 28]. During the tests, constant combustion center 9°CA aTDC (angle of 50% heat release) was maintained. Combustion of the hydrogen-ammonia mixture resulted in lower cylinder pressure, due to the lower total calorific value of the fuel and a different global excess air ratio. Despite a slightly higher fuel mass dose and a lower λ value at constant injection time settings, the combustion process deteriorated, resulting in lower maximum combustion pressures in both chambers.

Combustion at an excess air ratio $\lambda \approx 2$ resulted in significant pressure changes in the cylinder as the fuel dose to the prechamber increased, regardless of the fuel type. At higher λ values, pressure changes during hydrogen combustion remained significant, whereas in the $H_2 + NH_3$ mixture, they were lower in both the prechamber and the main chamber. This phenomenon is partly due to the low laminar combustion velocity of ammonia.

5.2. Analysis of combustion parameters

Engine performance indicators are shown in Fig. 7. Analysis of indicated pressure for different air excess ratios reveals different engine operating conditions for different fuels and fuel doses to the PC. Equal injection timing settings resulted in lower air excess ratios during combustion of $H_2 + NH_3$ (Fig. 7a), mainly due to changes in the injected fuel mass.

The analysis showed an increase in IMEP values due to higher fuel dose supplied to the prechamber. In each case analyzed, regardless of fuel type, an increase in IMEP of approximately 2% was observed (Fig. 7b).

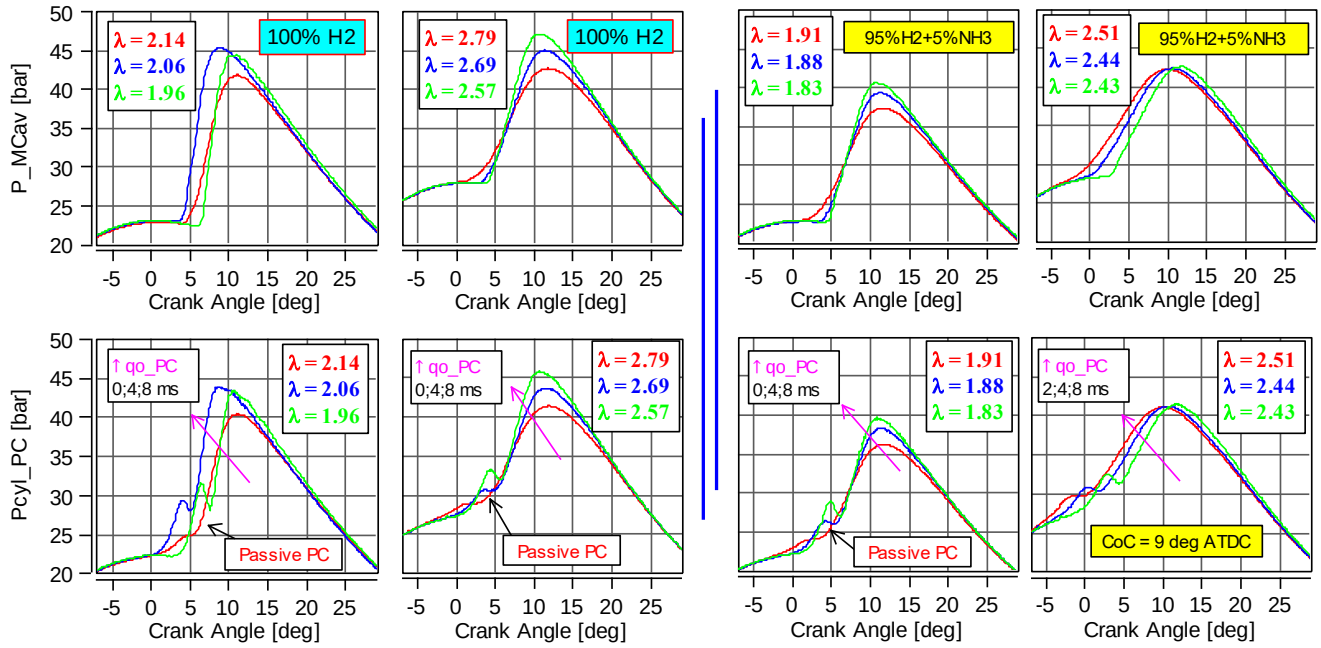

Fig. 6. Engine test results: indicator tests of the combustion process of hydrogen (left) and a hydrogen-ammonia mixture in a ratio of 95%/5% (right) at different excess air ratios

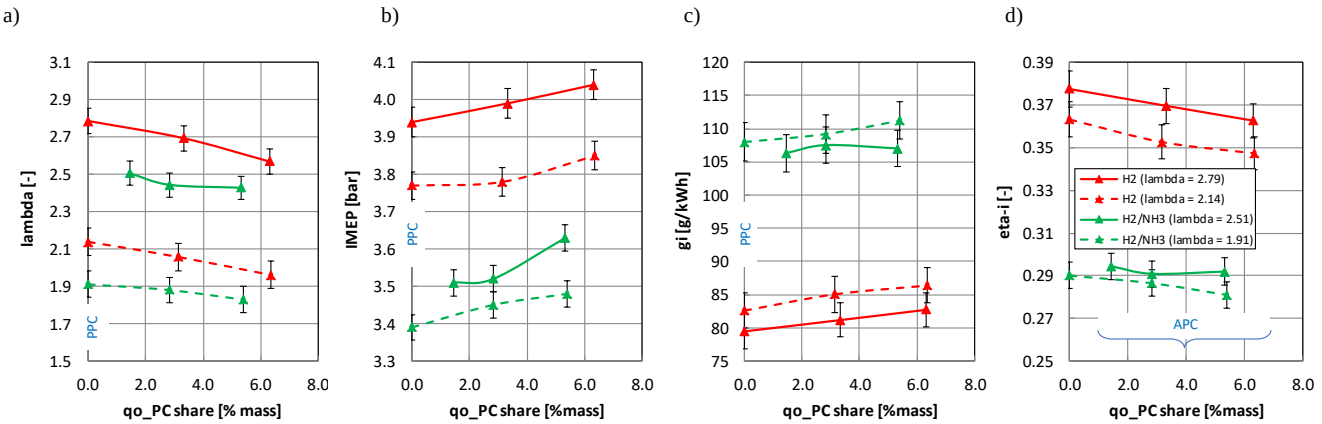

Fig. 7. Performance indicators for engines fuelled with hydrogen and hydrogen-ammonia: a) λ -value; b) IMEP; c) specific fuel consumption; d) indicating efficiency

Increasing the fuel dose to the prechamber also increased specific fuel consumption (Fig. 7c). Although the ammonia content in the mixture was only 5% by mass, the increase in specific fuel consumption reached approximately 4% compared to the passive chamber configuration. The difference in specific fuel consumption between hydrogen and an H_2 + NH_3 mixture exceeded 30%.

The analysis of the indicated engine efficiency showed significantly higher values with hydrogen (approximately 38%) than with a hydrogen-ammonia mixture (approximately 29%). This corresponds to a relative efficiency difference of 22% in favor of hydrogen (Fig. 7d). The results indicate that even a small mass addition of ammonia results in a significant deterioration in the performance of an engine with a two-stage combustion system.

6. Analysis of exhaust gas compositions

The combustion of hydrogen and its mixture with ammonia leads to significantly different concentrations of gaseous components in the exhaust gases (Fig. 8a). The combustion of pure hydrogen was characterized by relatively low concentrations of nitrogen oxides, ranging from about 30 ppm to over 300 ppm at higher excess air ratios, which is typical for the combustion of lean mixtures. The use of a 5% mass addition of ammonia resulted in a more than tenfold increase in NO_x concentration in the exhaust gases, due to nitrogen in the fuel and the intensification of the Fuel NO_x mechanism, with the simultaneous participation of the thermal (Zeldovich) mechanism.

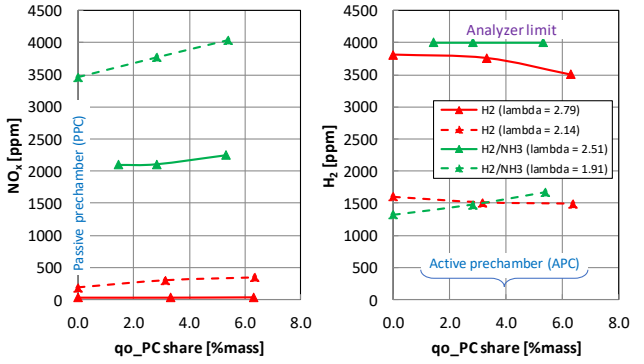

Fig. 8. The effect of variable fuel dose on the concentration of: a) nitrogen oxides; b) unburned hydrogen

Analysis of the unburned hydrogen concentration (Fig. 8b) shows an increase at high excess air ratios. Under the same conditions, using hydrogen or an H_2 + NH_3 mixture did not result in significant differences in unburned hydrogen emissions.

7. Analysis of particulate matter emissions

Analysis of particulate emissions in a hydrogen-fuelled engine indicates that their main source is lubricating oil entering the combustion chamber. Under low-load conditions, increased vacuum behind the throttle valve increases oil evaporation, which is then transported to the cylinder, leading to increased particulate emissions. In addition, at lower operating temperatures, the piston-ring-cylinder components undergo less thermal deformation, which increases oil leakage into the combustion chamber. As the load increases, improved sealing of the piston-ring-cylinder system reduces oil consumption, thereby lowering emissions and particulate matter [1, 2, 29].

Analysis of the particulate matter distribution (Fig. 9) indicates that the combustion of different carbon-free fuels has little effect on the shape of the particulate matter number. Regardless of the fuel type, the highest particle count was observed with a passive prechamber, with the distribution peaking at approximately 100 nm. This phenomenon can be associated with lower combustion efficiency in this configuration. The use of an active prechamber led to improved combustion quality and reduced particulate matter emissions.

In hydrogen combustion, at low air excess ratios, prechamber activation reduced particulate matter by approximately 35% (Fig. 9a).

During the combustion of lean hydrogen mixtures ($\lambda \approx 2.8$), the number of particles decreased from approximately 6×10^5 cm^{-3} with a diameter of 100 nm to approximately 5×10^5 cm^{-3} (Fig. 9b). Similar relationships were also observed during the combustion of a hydrogen-ammonia mixture (Fig. 9c and 9d). Increasing the fuel dose fed into the prechamber reduced the maximum number of particles. In addition, an increase in the excess air ratio caused a shift in the particle number distributions towards smaller diameters.

Research carried out by Apicella et al. [1] on a single cylinder 255 cm³ hydrogen fuelled engine (λ = 1.6; n = = 2000 rpm) showed similar values of particulate matter in the order of 1.0×10^6 cm^{-3} with an average diameter of

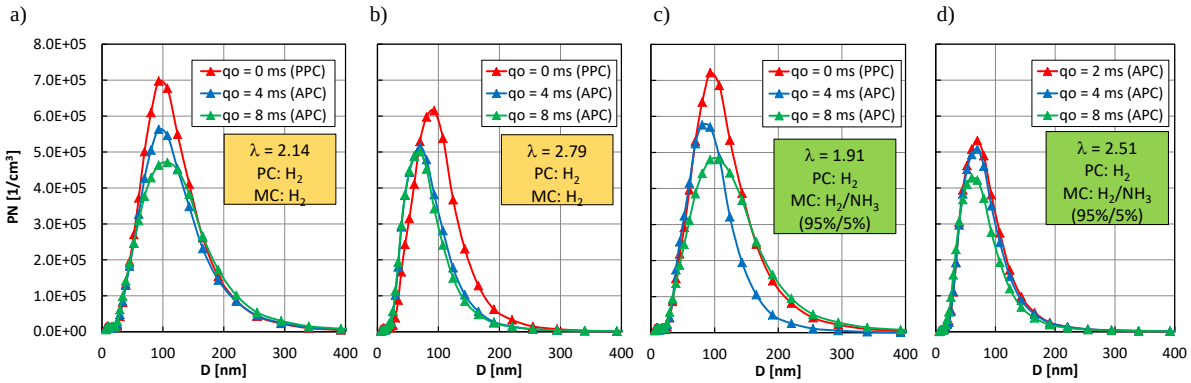

Fig. 9. Analysis of the number of particulate matter during combustion of hydrogen and a mixture of hydrogen and ammonia: a) λ = 2.15, hydrogen; b) λ = 2.79, hydrogen; c) λ = 1.65, hydrogen + ammonia; d) λ = 2.56, hydrogen + ammonia

approximately 39 nm under low engine load conditions (IMEP = 4.1 bar). At higher loads (IMEP = 5.5 bar; λ = 1.5), a further reduction in the number of particulate matter to approximately 1.0 × 10^4 cm^{-3} was observed, with a diameter of 10 nm.

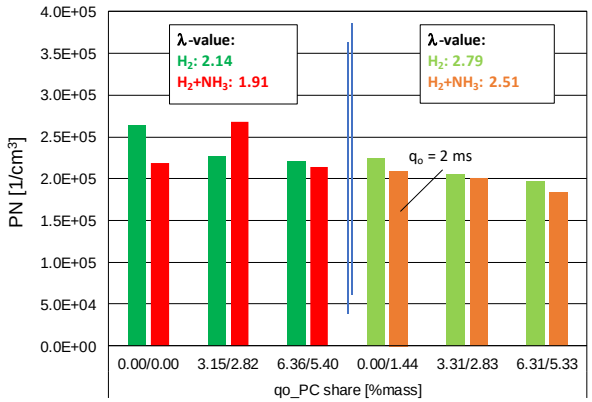

Fig. 10. Analysis of the number of particulate matter

Shi et al. [29], in their research on a single cylinder engine with a capacity of 604 cm^3 (n = 3000 rpm) with direct hydrogen injection (λ = 2.1), obtained a number of particles in the range from 1 × 10^6 to 5 × 10^6 cm^{-3}, depending on the engine operating conditions of 3 and 1 MPa. These results differ from those obtained in the current studies mainly in the reported maximum diameters (7–10 nm). This may mainly be due to differences in engine speed.

Figure 10 shows the values of the number of particulate matter obtained under engine operating conditions without the use of exhaust gas treatment systems. Analysis of combustion with hydrogen (λ = 2.14) and H_2 + NH_3 mixture (λ = 1.91) fuel indicates slightly higher values of the number of particles, ranging from (2.0–2.5) × 10^5 $1/cm^3$.

At higher excess air ratio values, the number of particulate matter stabilized at around 2.0 × 10^5 $1/cm^3$. The results show that, under the conditions analyzed, the type of carbon-free fuel has little effect on the number of particulate matter emitted.

Conclusions

The combustion of carbon-free fuels is an effective substitute for fossil fuels, especially in two-stage combustion systems in high excess air ratio conditions. Under the investigated operating conditions, hydrogen combustion provided the highest indicated efficiency (38% in current studies – Fig. 7d), while ammonia co-combustion has an efficiency of around 28%. These values were obtained at low engine loads, which indicates the significant potential of these fuels.

The detailed conclusions regarding combustion are as follows:

– The addition of ammonia reduces combustion pressure, which is due to the significantly lower energy content of the mixture
– Adding 5% ammonia to hydrogen reduces IMEP by approximately 10%, regardless of the load
– The addition of ammonia reduces the calorific value of the load, resulting in an increase in the specific fuel consumption of such a mixture by approximately 25%
– A small addition of ammonia causes a sharp increase in the concentration of NO_x in the exhaust gas: from 30 ppm (hydrogen at various values of λ) to over 2000 ppm when burning a mixture containing ammonia.

Analysis of particulate matter indicates that the largest source is engine oil, as changing the fuel has only a minor effect on their levels. Furthermore, it was found that increasing the lean ratio of the fuel-air mixture (hydrogen or a hydrogen-ammonia mixture) has little effect on particulate matter levels.

Nomenclature

APC	active prechamber
g_i	specific fuel consumption
IMEP	indicated mean effective pressure
MC	main chamber
NH_3	ammonia
N_i	indicated power
PC	prechamber
PN	particle number
PPC	passive prechamber
q_o	fuel dose
SI	spark ignition
TJI	turbulent jet ignition
λ	lambda value
η_i	indicated efficiency

Bibliography

[1] Apicella B, Catapano F, Di Iorio S, Magno A, Russo C, Sementa P et al. Comprehensive analysis on the effect of lube oil on particle emissions through gas exhaust measurement and chemical characterization of condensed exhaust from a DI SI engine fueled with hydrogen. Int J Hydrog Energy. 2023;48:22277-22287. https://doi.org/10.1016/j.ijhydene.2023.03.112

[2] Apicella B, Catapano F, Di Iorio S, Magno A, Russo C, Sementa P et al. Impact of fuel and lubricant oil on particulate emissions in direct injection spark ignition engines: A comparative study of methane and hydrogen. Fuel Process Technol. 2024;265:108144. https://doi.org/10.1016/j.fuproc.2024.108144

[3] Cova-Bonillo A, Gabana P, Khedkar N, Brinklow G, Wu M, Herreros JM et al. Predicting NO_x emissions from ammonia engines – fuel and thermal effects. Int J Hydrog Energy. 2025;187:150734. https://doi.org/10.1016/j.ijhydene.2025.150734

[4] Das L. Hydrogen-oxygen reaction mechanism and its implication to hydrogen engine combustion. Int J Hydrog Energy. 1996;21:703-715. https://doi.org/10.1016/0360-3199(95)00138-7

[5] Fenech A, Portelli S, Pipitone E, Farrugia M. Combustion characterization and heat loss determination through experimental investigation of hydrogen internal combustion engine. Energies. 2026;19:1424. https://doi.org/10.3390/en19061424

[6] Gu H, Ren F, Nakaya S, Tsue M. A comprehensive experimental and numerical study on turbulent jet ignition mechanisms of lean hydrogen mixture using a super-rich prechamber combustion. Combust Flame. 2025;279:114286. https://doi.org/10.1016/j.combustflame.2025.114286

[7] Guibert P, Tran K-H, Sebai S, Perceau M, Guilain S. Numerical simulation of predictive combustion and NO_x emissions for different ammonia/hydrogen fuels in SI engine using zero-1 dimensional thermodynamic modeling. Int J Hydrog Energy. 2025;143:500-512. https://doi.org/10.1016/j.ijhydene.2025.03.007

[8] Hong C, Xu S, Zhao S, Zhang H, Su F, Wang S et al. Analysis of ammonia as a combustion inhibitor for combustion knock and power expansion in a DI hydrogen engine. Fuel. 2024;375:132481. https://doi.org/10.1016/j.fuel.2024.132481.

[9] Iverach D, Basden KS, Kirov NY. Formation of nitric oxide in fuel-lean and fuel-rich flames. Symp Int Combust. 1973; 14:767-775. https://doi.org/10.1016/S0082-0784(73)80071-2

[10] Jeelan Basha KB, Balasubramani S, Sivasankaralingam V. Effect of pre-chamber geometrical parameters and hydrogen enrichment on the combustion and flame characteristics of zero/low carbon fuels. Energy. 2025;326:136365. https://doi.org/10.1016/j.energy.2025.136365

[11] Ji C, Xin G, Wang S, Cong X, Meng H, Chang K et al. Effect of ammonia addition on combustion and emissions performance of a hydrogen engine at part load and stoichiometric conditions. Int J Hydrog Energy. 2021;46: 40143-40153. https://doi.org/10.1016/j.ijhydene.2021.09.208

[12] Lai F, Sun B, Wang X, Zhang D, Luo Q, Bao L. Research on the inducing factors and characteristics of knock combustion in a DI hydrogen internal combustion engine in the process of improving performance and thermal efficiency. Int J Hydrog Energy. 2023;48:7488-7498. https://doi.org/10.1016/j.ijhydene.2022.11.091

[13] Li X, Sun B, Zhang S, Bao L, Luo Q, Leach F et al. Investigations of combustion characteristics and mechanism of backfire-induced super-knock in a turbocharged hydrogen engine. Energy. 2024;312:133453. https://doi.org/10.1016/j.energy.2024.133453

[14] Liang Y, Xing K, Huang H, Ning D, Wang Y, Wang X. Investigation of knock combustion mechanism and injection angle optimization in a heavy-duty direct-injection hydrogen engine. Energy. 2025;335:138041. https://doi.org/10.1016/j.energy.2025.138041

[15] Luo L, Huang Z, Xu Y, Zou S, Wu B. Experimental study on the effect of ammonia on combustion and emission characteristics of a spark ignition engine fueled with hydrogen. ACS Omega. 2024;9:46339-46348. https://doi.org/10.1021/acsomega.4c07315

[16] Ma T, Feng W, Sun X, Chen G, Jing G. Numerical study of NO_x formation mechanism in ammonia-hydrogen compound fuel marine engines under varying conditions. Int J Hydrog Energy. 2024;91:1422-1434. https://doi.org/10.1016/j.ijhydene.2024.10.213

[17] Mogi Y, Oikawa M, Kichima T, Horiguchi M, Goma K, Takagi Y et al. Effect of high compression ratio on improving thermal efficiency and NO_x formation in jet plume controlled direct-injection near-zero emission hydrogen engines. Int J Hydrog Energy. 2022;47:31459-31467. https://doi.org/10.1016/j.ijhydene.2022.07.047

[18] Mounaïm-Rousselle C, Bréquigny P, Dumand C, Houillé S. Operating limits for ammonia fuel spark-ignition engine. Energies. 2021;14:4141. https://doi.org/10.3390/en14144141

[19] Pal A, Agarwal AK. Hydrogen for internal combustion engines. In: Singh AP, Agarwal RA, Agarwal AK, Dhar A, Shukla MK (eds). Prospects Altern Transp Fuels. Springer. 2018:39-54. https://doi.org/10.1007/978-981-10-7518-6_4

[20] Pandey JK, Dinesh MH, Kumar GN. A comparative study of NO_x mitigating techniques EGR and spark delay on combustion and NO_x emission of ammonia/hydrogen and hydrogen fuelled SI engine. Energy. 2023;276:127611. https://doi.org/10.1016/j.energy.2023.127611

[21] Patil TS, Voris AR, Kane SP, Northrop WF. Ammonium nitrate nanoparticle emissions from ammonia-fueled internal combustion engines. J Aerosol Sci. 2025;188:106614. https://doi.org/10.1016/j.jaerosci.2025.106614

[22] Piano A, Pucillo F, Millo F, Giordana S, Rapetto N, Schuette C. Experimental investigation on the optimal injection and combustion phasing for a direct injection hydrogen-fuelled internal combustion engine for heavy-duty applications. Int J Hydrog Energy. 2025;100:398-406. https://doi.org/10.1016/j.ijhydene.2024.12.194

[23] Pielecha I, Szwajca F, Skobiej K, Pielecha J, Merkisz J, Cieślik W. Analysis on monofuel: methane and hydrogen in passive TJI engine using center of combustion and lambda-value control. Int J Hydrog Energy. 2024;83:1170-1183. https://doi.org/10.1016/j.ijhydene.2024.08.159

[24] Pyrc M, Gruca M, Tutak W, Jamrozik A. Assessment of the co-combustion process of ammonia with hydrogen in a research VCR piston engine. Int J Hydrog Energy. 2023;48: 2821-2834. https://doi.org/10.1016/j.ijhydene.2022.10.152

[25] Qiang Y, Cai X, Xu S, Wang F, Zhang L, Wang S et al. Effect of injection strategy on the hydrogen mixture distribution and combustion of the hydrogen-fueled engine with passive pre-chamber ignition under lean burn condition. Fuel. 2024;375:132610. https://doi.org/10.1016/j.fuel.2024.132610

[26] Qiang Y, Zhai Y, Xiang J, Yang J, Wang S, Ji C. Optimizing hydrogen direct injection strategy in a passive pre-chamber turbulent jet ignition NH_3/H_2 Miller-cycle engine: analysis of flow, combustion and emission characteristics. Energy. 2025; 332:137226. https://doi.org/10.1016/j.energy.2025.137226

[27] Qiang Y, Zhao S, Yang J, Cai J, Su F, Wang S et al. Effect of excess air ratio and spark timing on the combustion and emission characteristics of turbulent jet ignition direct injection hydrogen engine. Int J Hydrog Energy. 2024;93:1166-1178. https://doi.org/10.1016/j.ijhydene.2024.11.052

[28] Sementa P, De Vargas Antolini JB, Tornatore C, Catapano F, Vaglieco BM, López Sánchez JJ. Exploring the potentials of lean-burn hydrogen SI engine compared to methane operation. Int J Hydrog Energy. 2022;47:25044-25056. https://doi.org/10.1016/j.ijhydene.2022.05.250

[29] Shi W, Li Z, Dong W, Sun P, Yu X, Yang S et al. Effect of pre-combustion chamber hydrogen injection strategy on emissions and fuel economy of jet ignition engines under ultra lean-burn conditions. Int J Hydrog Energy. 2025;113: 147-160. https://doi.org/10.1016/j.ijhydene.2025.02.421

[30] Stępień Z. Analysis of the prospects for hydrogen-fuelled internal combustion engines. Combust Engines. 2024;197: 32-41. https://doi.org/10.19206/CE-174794

[31] Stępień Z, Urzędowska W. Hydrogen fuelled internal combustion engines – challenges. Nafta-Gaz. 2021;77:830-840. https://doi.org/10.18668/NG.2021.12.06

[32] Wang Z, Zhang T, Wang D, Wang S, Ji C, Wang H et al. A comparative study on the premixed ammonia/hydrogen/air

combustion with spark ignition and turbulent jet ignition. Energy. 2024;307:132814. https://doi.org/10.1016/j.energy.2024.132814

[33] Xin G, Ji C, Wang S, Meng H, Chang K, Yang J. Effect of different volume fractions of ammonia on the combustion and emission characteristics of the hydrogen-fueled engine. Int J Hydrog Energy. 2022;47:16297-16308. https://doi.org/10.1016/j.ijhydene.2022.03.103

[34] Xin G, Ji C, Wang S, Meng H, Chang K, Yang J. Effect of ammonia addition on combustion and emission characteristics of hydrogen-fueled engine under lean-burn condition. Int J Hydrog Energy. 2022;47:9762-9774. https://doi.org/10.1016/j.ijhydene.2022.01.027

[35] Zhou L, Liu P, Zhong L, Feng Z, Wei H. Experimental observation of lean flammability limits using turbulent jet ignition with auxiliary hydrogen and methane in pre-chamber. Fuel. 2021;305:121570. https://doi.org/10.1016/j.fuel.2021.121570

[36] Zhou L, Zhong L, Liu Z, Wei H. Toward highly-efficient combustion of ammonia–hydrogen engine: prechamber turbulent jet ignition. Fuel. 2023;352:129009. https://doi.org/10.1016/j.fuel.2023.129009

Dawid Mielcarzewicz, MEng. – Faculty of Civil and Transport Engineering, Poznan University of Technology, Poland.
e-mail: *dawid.mielcarzewicz@doctorate.put.poznan.pl*

Prof. Ireneusz Pielecha, DSc., DEng. – Faculty of Civil and Transport Engineering, Poznan University of Technology, Poland.
e-mail: *ireneusz.pielecha@put.poznan.pl*

Filip Szwajca, DEng. – Faculty of Civil and Transport Engineering, Poznan University of Technology, Poland.
e-mail: *filip.szwajca@put.poznan.pl*